Exp Brain Res (2001) 140:345–356
DOI 10.1007/s002210100832

RESEARCH ARTICLE

I. Telkes · N. Garipis · K.-P. Hoffmann

Morphological changes in the neuronal substrate for the optokinetic reflex in albino ferrets

Received: 20 November 2000 / Accepted: 11 June 2001 / Published online: 4 August 2001

Abstract Albino mammals show very characteristic deficits in their optokinetic system, and albino ferrets are even optokinetically blind. To investigate the neuronal causes for this defect we compared the morphology of retinal slip cells in the pretectal nucleus of the optic tract and the dorsal terminal nucleus of the accessory optic system (NOT-DTN) in pigmented and albino ferrets (*Mustela putorius furo*) using retrograde tracing techniques. After tracer injections into the inferior olive, equal numbers of NOT-DTN neurons were retrogradely labelled in pigmented and albino animals. However, NOT-DTN cells in albino ferrets had fewer stem dendrites, and the cumulative dendritic length was reduced by 30% when compared with NOT-DTN neurons in pigmented animals. In addition, the prominent network formed by distal dendrites observed in the NOT-DTN of pigmented ferrets was largely diminished in albinos. Taken together with behavioural and physiological data, these findings indicate that the NOT-DTN as the main visuomotor interface in the optokinetic system is clearly defective in albino ferrets.

Keywords Nucleus of the optic tract · Dorsal terminal nucleus · *Mustela putorius furo* · Retrograde tracing · Optokinetic nystagmus

Introduction

The pretectal nucleus of the optic tract (NOT) and the dorsal terminal nucleus of the accessory optic system (DTN) are primary visual centres playing an essential role in the generation of slow phase eye movements during horizontal optokinetic nystagmus (hOKN). Retinal slip neurons in these two adjacent structures cannot be distinguished based either on their response properties or on their anatomical connections. Thus, we consider them as a functional unit in the optokinetic reflex called NOT-DTN.

Electrical stimulation of the NOT-DTN elicits conjugate optokinetic eye movements, with the slow phase directed towards the stimulated hemisphere (rabbit: Collewijn 1975a; cat: Hoffmann and Fischer 2001; monkey: Schiff et al. 1988). After NOT-DTN lesions, hOKN can no longer be induced visually towards the lesioned side (rat: Cazin et al. 1980; rabbit: Collewijn 1975b; cat: Precht and Strata 1980; Hoffmann and Fischer 2001; monkey: Kato et al. 1986; Schiff et al. 1990; Ilg et al. 1993).

Frontal-eyed mammals such as cats and primates have a symmetrical optokinetic nystagmus, i.e. they respond equally well to both horizontal directions of stimulus movement during monocular viewing (Wood et al. 1973; Zee et al. 1987). Even though the eyes in ferrets are not as frontal as in cats, their visual system including their optokinetic nystagmus is strikingly similar to that of the cat (e.g. Greiner and Weidman 1981; Law et al. 1988; Hein et al. 1990). The symmetry of OKN is attributed to a binocular input from the visual cortex to the NOT-DTN (Wood et al. 1973; Hoffmann 1982), which enables each eye to drive either NOT-DTN. In the left NOT-DTN, neurons involved in the control of optokinetic reflex (OKR) are direction selectively activated by large visual stimuli moving to the left, whereas neurons in the right NOT-DTN prefer movement to the right. These neurons have been termed “retinal slip neurons” because they respond most strongly to the slip of the entire retinal image (Ballas and Hoffmann 1985). This functional organization of the NOT-DTN seems to be identical in all mammals, as substantiated by the results from receptive field analyses in a wide range of species (for a review of the literature see Grasse and Cynader 1990; Wallman 1993; Ibbotson et al. 1994; Hoffmann et al. 1995).

Retinal afferents to these neurons arise from direction selective ganglion cells (rabbit: Oyster et al. 1972; cat: Hoffmann and Stone 1985; for review see: Simpson

I. Telkes · N. Garipis · K.-P. Hoffmann (✉)
Allgemeine Zoologie und Neurobiologie,
Ruhr-Universität Bochum, Postfach 102148, 44780 Bochum, Germany
e-mail: kph@neurobiologie.ruhr-uni-bochum.de
Tel.: +49-234-3224363, Fax: +49-234-3214185

1984). The output of retinal slip cells in the NOT-DTN is sent to the dorsal cap and the nucleus beta of the ipsilateral inferior olive (IO) and other brainstem nuclei related to oculomotor functions (rat: Terasawa et al. 1979; rabbit: Takeda and Maekawa 1976; Holstege and Collewijn 1982; cat: Hoffmann et al. 1976; Itoh 1977; Magnin et al. 1989; monkey: Hoffmann et al. 1988; Mustari et al. 1994; Büttner-Ennever et al. 1996a, 1996b).

It is well established that albino mammals show several anatomical abnormalities in the visual system, starting with a decreased number of ganglion cells in the central retina and an abnormal decussation pattern of retinal ganglion cell axons at the optic chiasm (Jeffery 1997). The reduction of the ipsilateral retinofugal projection and abnormal geniculocortical pathways have been documented in several albino carnivores (ferret: Guillery 1971; Cucchiaro and Guillery 1984; Huang and Guillery 1985; Morgan and Thompson 1985; Morgan et al. 1987; cat: Guillery and Kaas 1971, 1973; Hubel and Wiesel 1971; Montero and Guillery 1978). In particular ipsilateral retinal projections to the NOT-DTN and other nuclei of the accessory optic system (AOS) are very strongly diminished or absent in albino ferrets, whereas they have been demonstrated in normally pigmented strains of species with frontally placed eyes (cat: Ballas et al. 1981; ferret: Zhang and Hoffmann 1993).

Albino mammals show some remarkable characteristics in their optokinetic behaviour. If only the temporal retina is stimulated, OKN is either inverted (mouse: Mangini et al. 1985; rat: Precht and Cazin 1979; Lannou et al. 1982; Sirkin et al. 1985; rabbit: Collewijn et al. 1978; man: Collewijn et al. 1985) or it is altogether absent in certain mouse and rat strains (Precht and Cazin 1979; Mangini et al. 1985) and ferrets (Garipis and Hoffmann 1999). These latter animals appear optokinetically blind, i.e. movement of the entire retinal image does not elicit optokinetic stabilizing eye movements. Interestingly, an optokinetically blind, hypopigmented mutant (sable) has also been described in zebra fish (Neuhauss et al. 1999). Corresponding deficits have been found for direction selective neurons in the NOT-DTN of albino rabbits (Winterson and Collewijn 1981), albino rats (Lannou et al. 1982), and albino ferrets (Garipis and Hoffmann 1999) in that the selectivity for ipsiversive stimulus movement is lost. In some cases the direction selectivity in the nasal visual field is even inverted to preferring contraversive movement (Winterson and Collewijn 1981). Since in normal animals direction selectivity is present already in the retinal ganglion cells projecting to the NOT-DTN (Oyster et al. 1972; Hoffmann and Stone 1985; for review see Wallman 1993), it was suggested that differences in the ipsilateral retinal projection to the NOT-DTN in albinos could cause the inverted nystagmus in rabbits (Winterson and Collewijn 1981).

In this study, we investigate whether the functional deficits in an optokinetically blind animal like the albino ferret are reflected in the functional anatomy of the NOT-DTN. The reduction of the ipsilateral retinofugal projections in these animals is well documented (Cucchiaro and Guillery 1984; Morgan et al. 1987; Thompson 1990; Zhang and Hoffmann 1993). Utilizing the robust projection from the NOT-DTN to the dorsal cap of the IO, we compared the number and dendritic morphology of IO-projecting neurons in the NOT-DTN of pigmented and albino ferrets by retrograde tracing techniques. Our results show that this part of the neuronal substrate for optokinetic nystagmus, i.e. the IO projecting cells in the NOT-DTN, is present in albino ferrets. However, we observed morphological changes which might give a first clue about the alterations in the OKN system at this first stage after the retina.

Materials and methods

Animals

All experiments were approved by the local ethics committee and were carried out in accordance with the European Communities Council Directive of 24 November 1986 (S6 609 EEC) and NIH guidelines for care and use of animals for experimental procedures. The experiments were carried out on young adult (7–12 months old) age matched pigmented (n=4) and albino (n=4) ferrets (*Mustela putorius furo*) of both sexes that had been bred and raised in the animal facility of the Department of Zoology and Neurobiology at the Ruhr-University, Bochum. Prior to the anatomical experiments, the optokinetic nystagmus (OKN) of the animals had been tested behaviourally (Garipis and Hoffmann 1999). The data of these individuals were indistinguishable from the data of the rest of our population, i.e. albino ferrets showed no OKN whereas pigmented animals did.

Surgery and injections

The animals were initially sedated with 2 mg/kg acepromacine (Vetranquil) and anaesthetized with 15 mg/kg ketamine hydrochloride. After additional local anaesthesia with bupivacaine hydrochloride (Bupivacain RPR 0.5%) or prilocaine hydrochloride (Xylonest), the animals were placed in a stereotaxic instrument and the skin overlying the posterior part of the skull and neck was opened. The neck muscles were bluntly parted until the foramen occipitale magnum was visible. Then the dura mater was opened to reveal the obex of the fourth ventricle. The injections into the inferior olive (IO) were performed with a Hamilton syringe 1 mm lateral to the obex with the tip angled at 45° posterioanteriorly (complete method described by Horn and Hoffmann 1987). On both sides of the brain, either 0.25 µl horseradish peroxidase (HRP, 20% in distilled water containing 2% dimethylsulphoxide, DMSO), or in one of the albino animals 0.5 µl biocytin-dextran [Molecular Probes, MW 3000, 15% in 0.1 M NaOH citrate (pH 3) containing 2% DMSO], was slowly injected over 30 min. After an additional waiting period of 15 min, the syringe was withdrawn. In one pigmented and two albino animals only the right IO was injected. After completion of all injections, the dura opening was covered with Gelfoam (Gelita Tampon) and the wound was closed in appropriate layers. After complete recovery, the animals were returned to the animal quarters.

Histology

After a survival time of 36–72 h, the animals were again anaesthetized with 30 mg/kg ketamine and 0.1 ml xylazine hydrochloride (Rompun) and put to death with an overdose of pentobarbital. Then the animals were perfused through the heart with 0.9% NaCl containing 0.1% procaine hydrochloride followed by paraformaldehyde-lysine-periodate (PLP) containing 4% paraformaldehyde.

Table 1 Summary of experimental design

Case	IO injections	Reaction	Intensification	No. of labelled cells in the NOT-DTN	No. of labelled dendrites	Total length of dendrites (μm)
Pigm. 1	HRP, both sides	DAB	+	Left: 178 Right: 288 Total: 466	2199	21,311
Pigm. 2	HRP, both sides	TMB	–	Left: 76 Right: 83 Total: 159	1133	13,072
Pigm. 3	HRP, both sides	DAB	+	Left: 92 Right: 37 Total: 129	581	10,342
Pigm. 4	HRP, right side	DAB	+	Right: 449 Total: 449	1480	21,427
				Total: 1203	Total: 5393	Total: 66,152
Albino 1	HRP, both sides	DAB TMB	+ –	Left: 157 Right: 148 Total: 302	1328	12,036
Albino 2	Biocytin-dextran, both sides	Avidin conjugate ABC + DAB	+	Left: 36 Right: 98 Total: 134	512	4076
Albino 3	HRP, right side	DAB	+	Right: 240 Total: 240	1078	16,725
Albino 4	HRP, right side	DAB	+	Right: 282 Total: 282	966	13,578
				Total: 958	Total: 3884	Total: 46,415

Summary of tracers and visualization methods used, number of retrogradely labelled cells in the NOT-DTN, number of labelled dendrites, and total length of the dendrites in albino and pigmented animals. In the animals with bilateral tracer injections, we combined the number of labelled cells or labelled dendrites in the right NOT-DTN and the left NOT-DTN and called them the "total number" of labelled cells or labelled dendrites

The brain was removed from the skull. After postfixation overnight in PLP, the tissue was cryoprotected with 10% and 20% glycerin and 2% DMSO in 0.1 M phosphate buffer (PB; pH 7.4). The brain was blocked stereotaxically into one block including the midbrain and one block including the inferior olive, which were cut into 50-μm-thick frontal sections on a freezing microtome (Microm, HM 500 OM). Two alternate series were collected into 0.1 M PB saline (PBS, pH 7.6), one for visualizing the neuronal tracers, the other for identifying subcortical nuclei in Nissl-stained material.

The HRP was visualized using 3,3'-diaminobenzidine tetrahydrochloride (DAB) (see below) or 3,3',5,5'-tetramethylbenzidine (TMB) as a chromogen (Mesulam 1978, as modified after van der Wandt et al. 1997). In the case where biocytin-dextran was used, sections were treated with avidin conjugate (ABC-Elite, Vector) 1:250 in PBS overnight. This reaction product was visualized with a solution of 0.025% DAB (Sigma), 0.15% ammonium nickel sulphate (Fluka) and 0.003% H_2O_2 (Baker) in 0.1 M TRIS-HCl (pH 7.6). The same reaction was used to stabilize the TMB reaction product (modified by Horn and Hoffmann 1987). The end product was amplified with a gold-substituted silver intensification technique (Gallyas et al. 1993). This technique was slightly modified for optimal HRP visualization. After the DAB-Ni reaction, the tissue was washed twice for 10 min in 0.1 M TBS, then twice for 10 min in 1% sodium acetate. The sections were treated with 10 mM copper sulphate for 10 min and, after rinsing in 1% sodium acetate, with 3% H_2O_2 for an additional 10 min. Before the intensification, the tissue was rinsed in 1% sodium acetate again. The intensification was carried out in a freshly prepared solution of equal parts of 5% Na_2CO_3 + 0.1% $AgNO_3$ supplemented with 0.1% NH_4NO_3, 1% silicotungstic acid, and 0.25% formaldehyde for 2–6 min. Washing twice for 10 min in 1% acetic acid stopped the reaction. After rinsing in 1% sodium acetate, the sections were gold toned in 0.1% $HAuCl_4$ for 10 min, rinsed in 1% sodium acetate and treated with 3% $Na_2S_2O_3$ for 5 min. At the end of the reaction, the midbrain sections were washed in 1% sodium acetate, then mounted on gelatinized slides, dehydrated in increasing concentrations of ethanol, cleared in xylene and coverslipped with DEPEX. This procedure gave results highly superior to normal TMB or DAB reactions in that the labelled cells and neuropil were visualized in great detail and with minimal background. The sections were analysed using a Zeiss Axioskop microscope. The position and the morphology of single retrogradely labelled neurons were reconstructed with a camera lucida apparatus using a ×40 objective.

Quantitative analysis

Three pigmented and two albino ferrets received bilateral IO injections. In these animals we analyzed the right and the left NOT-DTN. One pigmented and two albino ferrets received IO injections only on the right side. Here we analysed only the right NOT-DTN. The number of retrogradely labelled neurons and their dendrites in the NOT-DTN were counted and the length of dendritic segments measured (Table 1). In this study we did not attempt to follow dendrites through adjacent sections. Only every second section was used for visualizing retrogradely labelled cells; the second series was used for Nissl staining for identification of pretectal nuclei. Each labelled neuron with a clearly distinguishable soma was reconstructed. Because of the intersection distance of 100 μm, it is unlikely that the same cell was analysed twice even if it was not sectioned mid-soma. The resulting drawings were scanned into a computer and the dendrites were measured by tracing them with the mouse on the computer screen. Only dendrites obviously connected to a soma were measured. If branching occurred, we followed the most clearly labelled branch. Dendritic fragments which could not be followed to a particular cell were not included in the

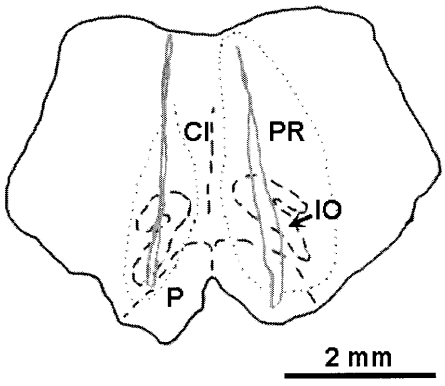

Fig. 1 Line drawing of typical injection sites in the brainstem of an albino ferret. The penetration tracks (*grey*) reached the inferior olive (*IO*) on both sides. *The dotted outlines* indicate the extent of the injections that include the inferior central nucleus (*CI*), the paramedian reticular nucleus (*PR*), and the pyramidal tract (*P*). *Scale bar* 2 mm

analysis. The number and length of the dendrites were quantified in sixteen 22.5°-wide sectors of a circle centred onto the soma of each cell, with the first sector being parallel to the superficial fibre layer and directed laterally. Soma size was not measured because the gradual transition between soma and dendrite often made a strict delineation of the soma impossible.

Results

Injection sites

We investigated retrogradely labelled NOT-DTN cells from four pigmented and four albino ferrets. The location of the injection site in the inferior olive, the tracer used, the method to visualize it, as well as the number of labelled NOT-DTN neurons, and the number and total length of the labelled dendrites in each animal are summarized in Table 1. The spread of the tracer at the injection sites in the brainstem had a core diameter varying between 300 and 500 µm and always included most of the inferior olive at least on one side (Fig. 1). In five cases left and right IO, and in three cases only the right IO, were covered by the tracer (Table 1). Sometimes other structures such as the medial longitudinal fasciculus, the paramedian reticular nucleus, the inferior central nucleus, and the pyramidal tract were also labelled. These injections resulted in extensive retrograde labelling of neurons in various areas of the midbrain. Retrogradely labelled neurons were found in the NOT-DTN, the medial terminal nucleus (MTN), the superior colliculus (SC), and the ventral tegmental relay zone (VTRZ). Especially in the cases with one-sided injections labelled NOT-DTN neurons ipsilateral to the injection were well separated from the neurons of other structures and were therefore easy to analyse. The labelling was independent of the type of tracer. Survival time also had no influence on labelling strength. The number of strongly labelled neurons was more dependent on the site of the injection in the IO than on tracer and survival time.

Number of cells in the NOT-DTN in albino and pigmented animals

The line drawings in Fig. 2 give an overview of the pretectal region in a pigmented (A) and an albino (D) ferret, the rectangular inset indicating the region depicted in the photomicrographs of Figs. 2B, C, E, F and 3. Within the pretectum, retrogradely labelled neurons were found mainly in the ipsilateral dorsal NOT-DTN just below the midbrain surface. A few labelled neurons were also observed in the ventral NOT-DTN, but their number steadily decreased more ventrally. The labelled cells were not organized in layers but were seen to be randomly dispersed in the NOT-DTN (Fig. 2). Despite the large injections centred at the caudal pole of the inferior olive near the dorsal cap, the variability in the number of labelled neurons was considerable. The average number of neurons labelled was 172 per NOT-DTN in the pigmented and 160 in the albino animals. This difference was neither statistically significant in a *t*-test nor in a non-parametric Mann-Whitney U-test.

Morphology of labelled cells in the NOT-DTN

Inspecting our histological material, well-labelled somata and a strongly stained dendritic network were observed in the NOT-DTN of all pigmented animals (arrowheads in Fig. 2B, C). Although the somata appeared equally well labelled in the albino ferrets, such a dendritic network was missing or it consisted of weakly stained, loosely arranged dendrites (arrows in Fig. 2E, F). Furthermore, it was conspicuous that NOT-DTN cells in pigmented animals seemed to have longer dendrites oriented mostly along the optical fibre layer parallel to the surface of the midbrain (Fig. 2B, C).

Figure 3 depicts retrogradely labelled neurons with well-filled somata and proximal dendrites in pigmented (Fig. 3A, B) and albino ferrets (Fig. 3C, D). The somata of these neurons displayed a wide range of sizes and shapes. Somata of IO-projecting neurons located dorsally were fusiform (Fig. 3A, C), whereas those located centrally or ventrally in the nucleus were fusiform to round (Fig. 3B–D). Some neurons at the dorsal and superficial border of the NOT-DTN had cell bodies with an elongated appearance (Fig. 3A). We did not attempt to

Fig. 2 Retrogradely labelled neurons in the right NOT-DTN after IO injections. *Line drawings in* **A** *and* **D** show an overview of the midbrain and pretectum of a pigmented **(A)** and an albino ferret **(D)**; *rectangles* indicate the region of the NOT-DTN shown in the photomicrographs in **B, C, E,** and **F**. **B, C** Typical labelling of the NOT-DTN in two pigmented animals after HRP injections. Note the strongly stained dendritic networks in the NOT-DTN of these animals (*arrowheads*). **E, F** Typical retrograde labelling in the NOT-DTN of two albino ferrets. The dendritic network is replaced by weakly stained, loosely arranged fibres in the albino NOT-DTN (*arrows*) (*A* aqueduct, *MGN* medial geniculate nucleus, *PAG* periaqueductal grey, *PP* pes pedunculi, *SC* superior colliculus, *III* oculomotor nucleus, *3* oculomotor nerve). *Scale bar* for photomicrographs represents 400 µm, for line drawings 2 mm

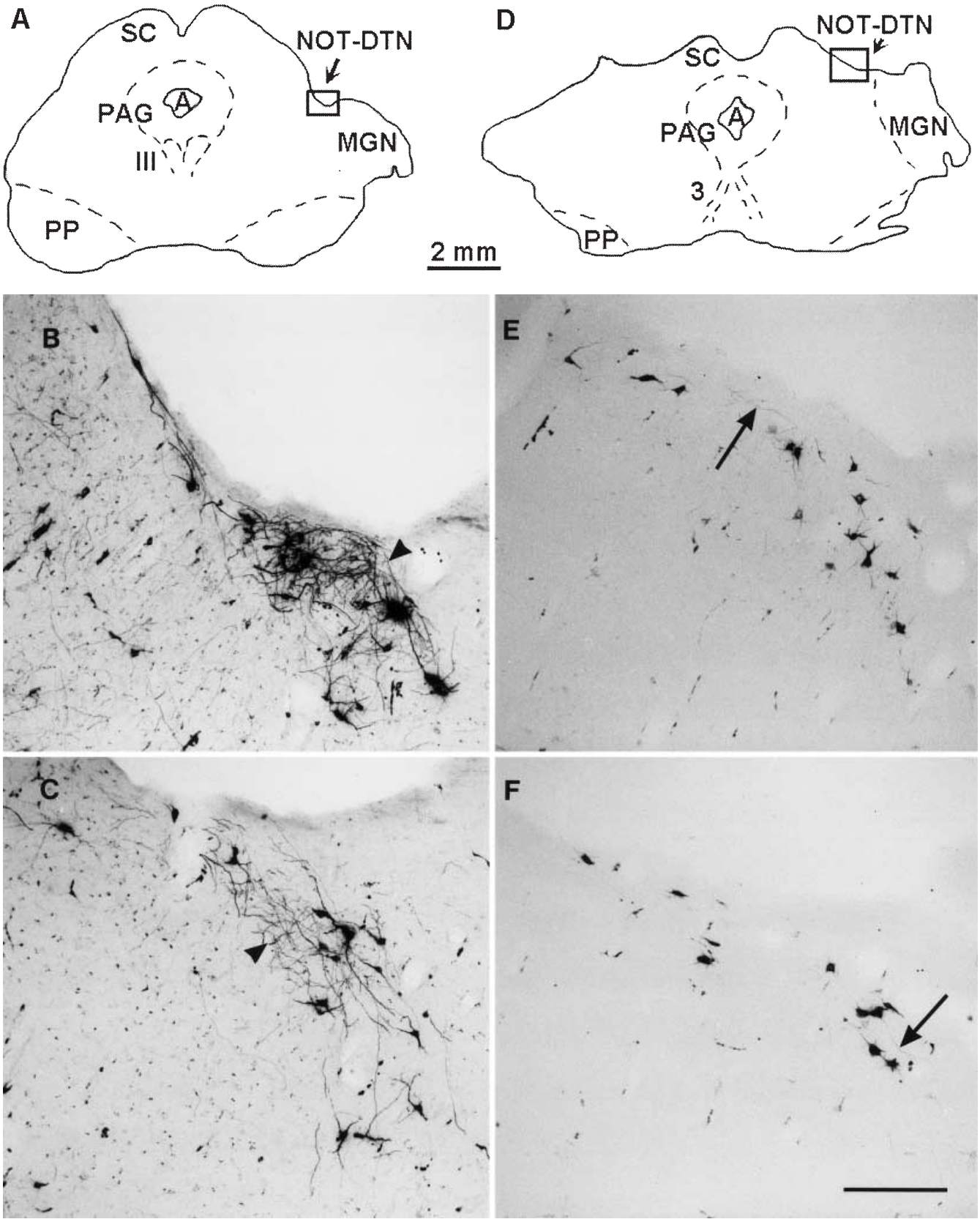
A
SC
NOT-DTN
PAG
A
III
MGN
PP
2 mm
D
NOT-DTN
SC
PAG
A
MGN
3
PP
B
E
C
F

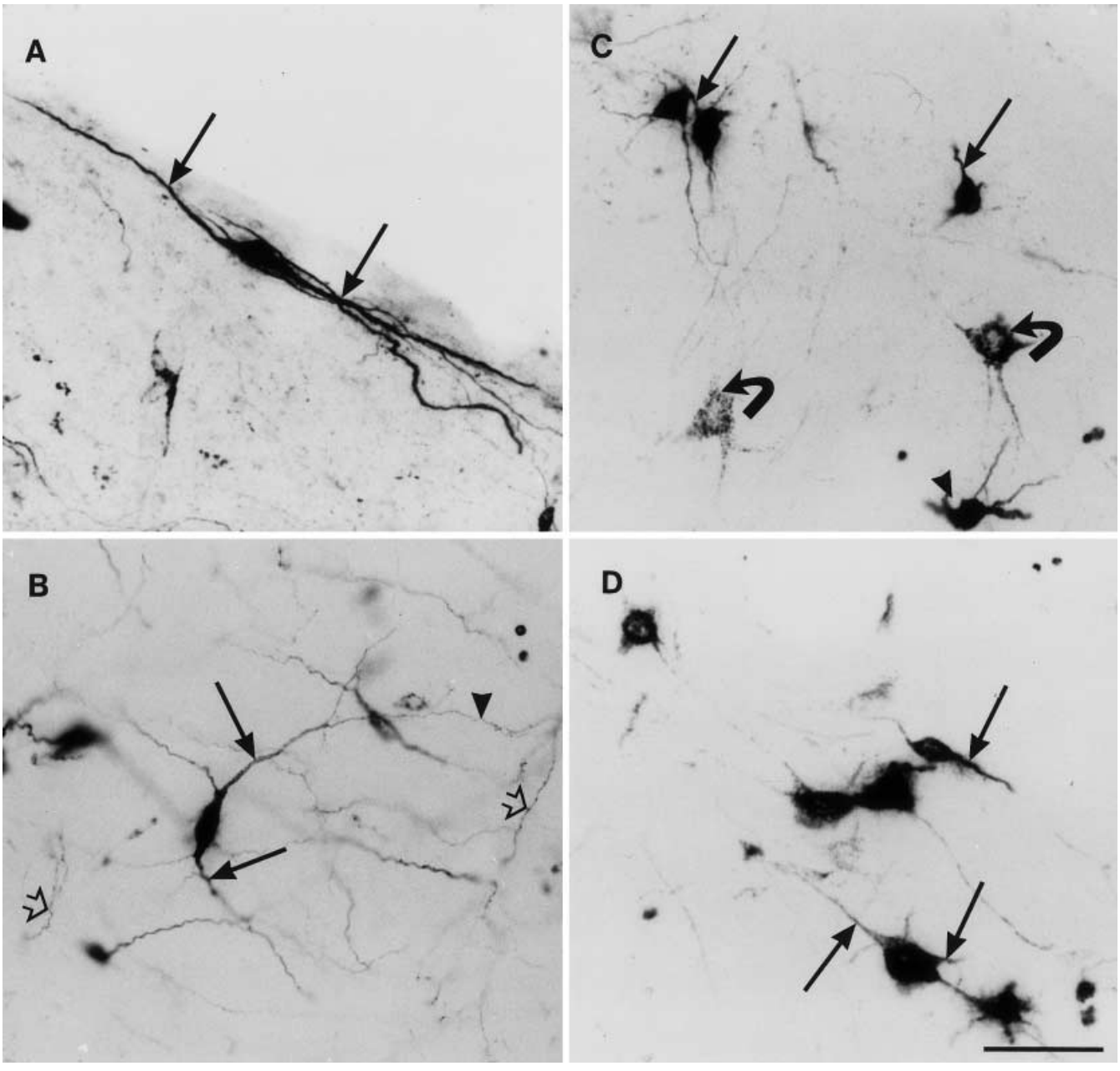

Fig. 3 Neuronal types in the NOT-DTN projecting to the IO of pigmented and albino ferrets as visualized by DAB reaction and gold-substituted silver intensification after HRP injections into the ipsilateral IO. **A** Strongly labelled neuron with a flattened soma at the dorsal border of the NOT-DTN in a pigmented ferret. The main dendrites (*arrows*) are well filled and can be followed up to 100 µm from the cell body. **B** Strongly labelled neuron from the central part of the NOT-DTN in a pigmented ferret with fusiform soma and well-filled main dendrites (*arrows*). The peripheral dendrites have a granular appearance (*arrowhead*), but the branching pattern can still be followed. Some parts of thin beaded dendrites, belonging to the strongly labelled dendritic network of the pigmented NOT-DTN, can be seen (*open arrows*). **C** Labelled neurons in the right NOT-DTN of an albino. *Solid arrows* point to stem dendrites of fusiform dorsal cells; *curved arrows* point to fusiform to round cells located more ventrally. The ventrally located neurons have dendrites extending into the central part of the NOT-DTN (*arrowhead*). **D** Retrogradely labelled fusiform to round cells in the central part of the NOT-DTN of an albino animal. The main dendrites are well filled (*arrows*) and extend in all directions of the NOT-DTN. *Scale bar* 50 µm

measure soma size because of this variable appearance and because it was often difficult to define the exact border between soma and dendrite. Qualitatively, there was no obvious difference in soma size between the two groups of animals.

Labelled neurons had two to seven stem dendrites that could be followed up to 100–140 µm from the middle of the cell body in the 50-µm-thick frontal sections (solid arrows in Fig. 3). Although the peripheral dendrites of these cells had a granular appearance, their branching pattern could still be distinguished (arrowhead in Fig. 3B). The dendritic branching pattern of labelled cells was found to depend on their position in the NOT-DTN. Neurons with elongated cell bodies situated dorsally in the NOT-DTN had dendrites that extended parallel to the surface of the midbrain or to the fibre

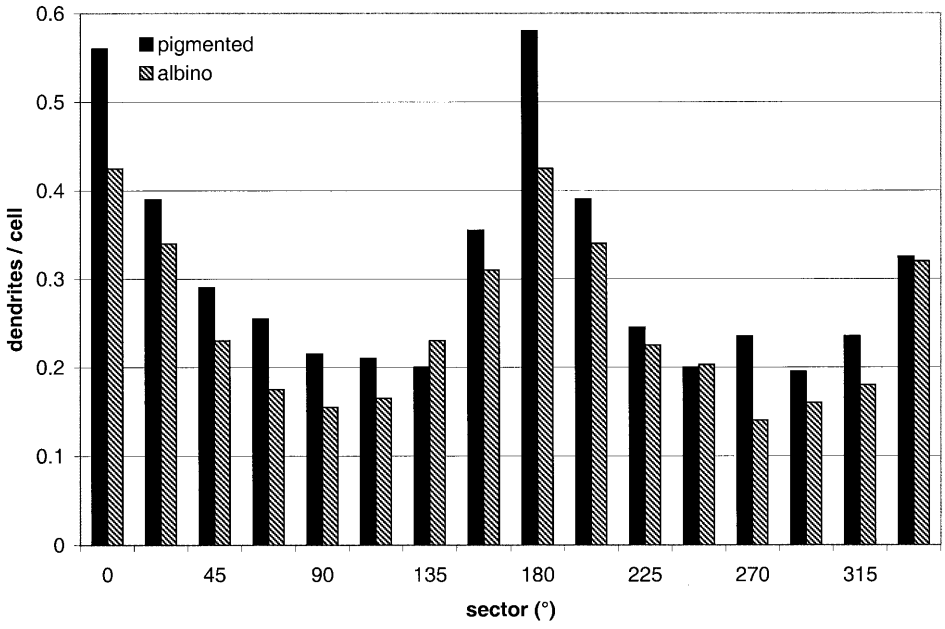

Fig. 4 Number of dendrites of labelled neurons in each orientation sector. The data are normalized to the total number of labelled cells for each animal and then averaged for each animal group. This measure gives us the average frequency of dendrites for one cell to fall in one of the sectors. *Abscissa* shows the 16 sectors (°); *ordinate* gives the frequency of dendrites per cell in a sector. Sector 0° always points laterally and sector 180° towards the midline of the midbrain. Overall, there are more dendrites in pigmented animals. In both groups of animals the highest frequency of labelled dendrites was found in the sectors parallel to the surface of the midbrain, i.e. parallel to the fibre bundles of the BSC

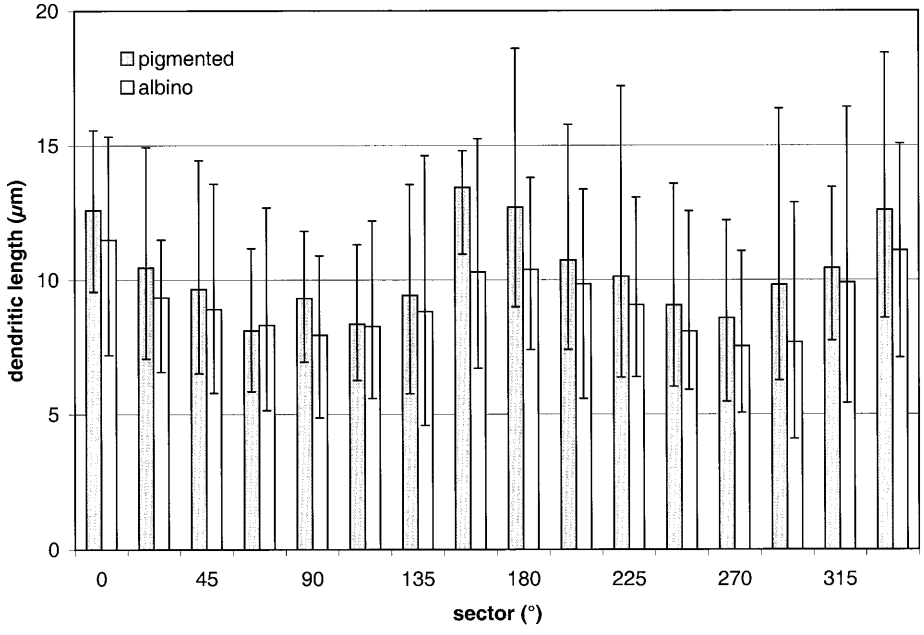

Fig. 5 Average of the medians of dendritic length in each sector in the two groups of animals. *Abscissa* orientation sectors (°), *ordinate* medians of dendritic length in micrometres. This median length of dendrites is still significantly shorter in albino than in pigmented ferrets. The median of the dendritic length is higher in the sectors parallel to the midbrain surface in each animal group. *Bars* give the maximum and minimum of the medians for each sector in each animal group

bundles of the brachium of the superior colliculus (BSC) (Fig. 3A). Ventrally, labelled neurons were found with dendrites that extended dorsally into the central parts of the NOT-DTN (arrowhead in Fig. 3C), while labelled neurons in the central part of the NOT-DTN branched in all directions (Fig. 3B, C). In general, the main dendritic orientation observed in transverse sections was parallel to the surface of the midbrain, i.e. parallel to the fibre bundles in the BSC. There was no obvious difference between pigmented and albino ferrets.

Overall, the dendrites of labelled neurons were restricted to the borders of the NOT-DTN which could be delineated from Nissl stained sections according to the criteria established by Zhang and Hoffmann (1993).

Quantitative analysis

To verify our qualitative observations on the dendrites in the pigmented and albino ferrets, we quantitatively analysed the following anatomical parameters: first, the average frequency of dendrites per cell in each sector (Fig. 4), second, the median of the dendritic length in each sector (Fig. 5) and, third, the cumulative length of dendrites in each sector per NOT-DTN (Fig. 6).

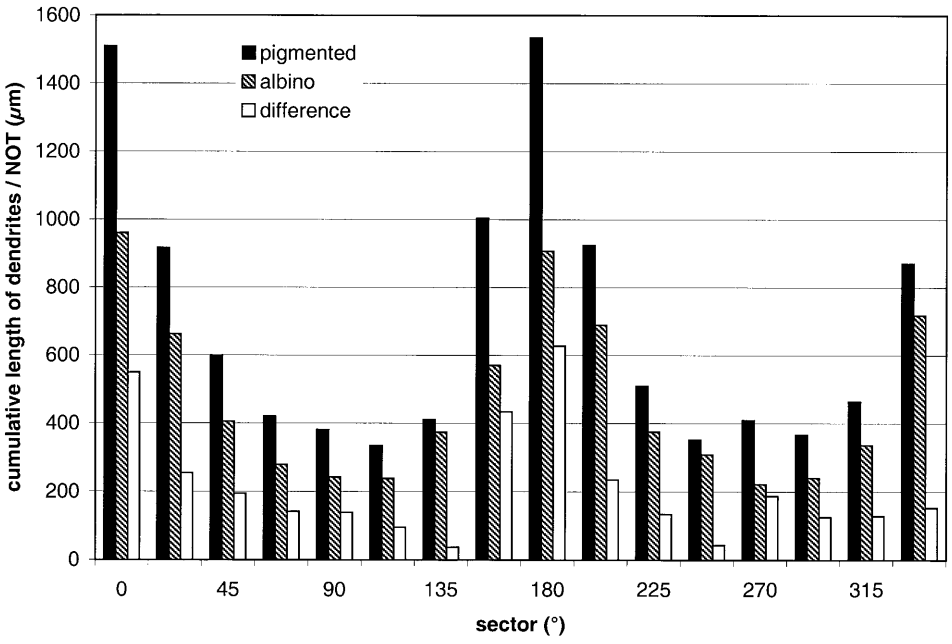

Fig. 6 Cumulative length of the dendrites in each sector averaged for the analysed NOT-DTNs. *Abscissa* orientation sectors (°), *ordinate* cumulative dendritic length per NOT-DTN in each sector of the two groups of animals. The cumulative dendritic length is dramatically but evenly decreased by about 30% in albino compared with pigmented ferrets. The dendritic length per NOT-DTN is highest in the sectors parallel to the midbrain surface in both animal groups

The number of dendrites analysed per animal and NOT-DTN is given in Table 1. The average number of dendrites per cell was derived by dividing the number of dendrites in all sectors by the number of cells analysed for each animal. The average number of dendrites originating from the soma ranged from 3.3 to 7.1 in pigmented and from 3.4 to 4.5 in albino animals. We counted the total number of labelled dendrites in each sector separately and normalized the values to the number of cells counted in the same sections for each pigmented and albino animal. From these values, we calculated the average probability of a cell in a pigmented animal to have a dendrite in any sector to be 0.3, in the sectors parallel to the fibre layer (0° and 180°) to be 0.57. In the albino animals these probabilities were 0.25 and 0.42, respectively. Figure 4 shows the clearly decreased average frequency of dendrites from albino animals in almost all of the investigated sectors in comparison to the pigmented animals. Over the 16 sectors, this difference is highly significant in a Wilcoxon signed rank test ($P<0.001$). There is no greater loss of dendrites in the sectors parallel to the fibre layer (0° and 180°) in the albino animals when compared with other sectors.

Next, we calculated the median length of dendrites in a given sector for each labelled cell (Fig. 5). Most of the dendritic segments were short, in part because we did not reconstruct dendrites over consecutive sections. Thus, each dendritic segment was measured separately and the median of the values calculated in each sector in every animal. The maximum and minimum of the medians in the 16 sectors were smaller in the albino animals (16.43 µm and 4.09 µm vs 18.43 µm and 5.47 µm in pigmented animals, Fig. 5). The mean of the medians over all 16 sectors in each animal group was only slightly shorter in albino animals (9.18±1.67 µm vs 10.34± 1.2 µm in pigmented animals). Nevertheless, the difference in the medians between albino and pigmented strains was significant ($P<0.05$ in a *t*-test) and highly significant if the difference between the values in the 16 sectors was tested pairwise ($P<0.001$ in a Wilcoxon signed rank test). The median length of dendrites appeared slightly longer in the sectors parallel to the fibre layer than in other sectors in both of the animal groups [both distributions deviate significantly ($P<0.001$, χ^2-test) from a uniform distribution].

The clearest picture arises if the cumulative length of dendrites per NOT-DTN in each sector is compared for the pigmented and albino animals (Fig. 6). In the pigmented ferrets seven NOT-DTNs, in the albinos six NOT-DTNs, were analysed. To compensate for the differences in the number of labelled cells, we normalized the cumulative dendritic length in each sector to the number of labelled cells in each animal. This average cumulative dendritic length per sector (Fig. 6) was dramatically decreased in albino animals when compared with pigmented animals particularly in the sectors parallel to the fibre layer (0° and 180°). However, the relative decrease in cumulative dendritic length was about equal (30% shorter) in each sector of the albino animals when compared with the pigmented ones. This difference was not higher in the sectors parallel to the fibre bundles of the BSC. Thus, the labelled dendrites in the albino animals still have a preferred orientation parallel to the optical fibre layer.

In summary, we found equal numbers of NOT-DTN neurons projecting to the IO in pigmented and in albino ferrets. However, these cells had fewer dendrites in albino animals. The dendrites had similar orientations with respect to the surface of the midbrain, but the cumulative dendritic length was decreased by 30% in all directions in albino ferrets as compared to pigmented animals.

Discussion

In the present study we investigated the key neuronal substrate for the optokinetic reflex in pigmented and albino ferrets. We concentrated on neurons in the NOT-DTN that project to the dorsal cap of the inferior olive and analysed their number and morphology using retrograde transport of HRP and biocytin coupled to dextran. Our data show that IO-projecting neurons are present in equal numbers in the NOT-DTN of both pigmented and albino ferrets. However, a detailed analysis revealed several morphological characteristics distinguishing the two groups of animals. First, qualitatively a very prominent dendritic network was evident in the NOT-DTN of pigmented but not of albino animals. Second, on average, IO-projecting neurons in the NOT-DTN of albino ferrets had fewer stem dendrites than in pigmented animals. Third, the orientation of the dendrites was similar in both pigmented and albino ferrets. However, the average dendritic length per cell was shorter in albino than in pigmented animals. Fourth, the cumulative dendritic length in the NOT-DTN of albinos was reduced by 30% when compared with pigmented animals.

Specificity of injection sites

Previous studies in rat, cat, and opossum indicate that there are several distinctive neuronal populations in the NOT-DTN. They can be distinguished by their response properties as well as their projection sites (Ballas and Hoffmann 1985; Magnin et al. 1989; Schmidt et al. 1995; Vargas et al. 1996). The neurons relevant for the optokinetic reflex are the direction selective retinal slip cells that project to the IO and, in part, by axonal bifurcation to the nucleus praepositus hypoglossi (Magnin et al 1989). Our injection sites were always centred in the IO, and although they included neighbouring structures, e.g. the pyramidal tract, the medial longitudinal fasciculus, and the paramedian reticular nucleus to a varying degree, none of these structures has been recognized as a NOT-DTN output target (rat: Terasawa et al. 1979; rabbit: Takeda and Maekawa 1976; Holstege and Collewijn 1982; Giolli et al. 1984; cat: Graybiel and Berson 1980; Walberg et al. 1981; Ballas and Hoffmann 1985; ferret: Zhang 1991; monkey: Mustari et al. 1994; Büttner-Ennever et al. 1996b). In addition, the labelled neurons in the NOT-DTN formed a cluster well separated from neighbouring structures such as the superior colliculus or other pretectal nuclei. Therefore, we are confident that only retinal slip cells projecting to the IO were included in our analysis. The variability in the total number of labelled neurons may in part be due to differences in the exact location of the injection centre, leakage of tracer out of the brainstem into the liquor, and uncontrollable differences in uptake and transport of the tracer.

Morphology of retrogradely labelled NOT-DTN neurons

Analysis of the morphology of retrogradely labelled neurons in the NOT-DTN revealed three types of neurons. The shape of the soma ranged from fusiform to round, the orientation of the stem dendrites ranged from parallel to the surface to undirected. These cell types were not well segregated from each other, nor was there a clear organization in morphological layers. Roughly, fusiform cells with surface parallel dendrites were located dorsally, fusiform to round cells with unoriented dendrites were located centrally, and fusiform to round cells with dorsally oriented dendrites were located ventrally in the NOT-DTN. This corresponds to data from rat and cat where the morphology of NOT-DTN neurons varies with their location within the nucleus rather than with their functional type as determined by their efferent projections (Gregory 1985; van der Togt and van der Want 1992; Schmidt et al. 1995). Ferret NOT-DTN cells projecting to the IO partly overlap with the terminal fields of the retinopretectal afferents (Zhang and Hoffmann 1993). Our analysis revealed that IO-projecting cells in the albino NOT-DTN have fewer stem dendrites, and the cumulative length of the dendrites per orientation sector was reduced by 30% when compared with normally pigmented animals. This suggests a possible decrease of inputs to these cells. No comparable data are available for hypopigmented mice, rats, rabbits, or cats. Electrophysiological data on antidromic latencies of NOT-DTN cells after electrical stimulation in the IO of pigmented and albino ferrets do not reveal statistically significant differences between the two groups of animals even though less neurons with very short antidromic latencies were found in albinos (Garipis and Hoffmann, unpublished observations). Thus, it is unlikely that a slightly thinner axon diameter of retinal slip cells in the NOT-DTN should significantly impair retrograde transport and as a consequence the quality and extent of dendritic labelling.

Functional considerations

The following key features characterize the optokinetic system of albino mammals. Behaviourally, albino mammals can show a reversal of the slow phase of optokinetic nystagmus when only the nasal visual field is stimulated (Collewijn et al. 1978, 1985; Sirkin et al. 1985). Some strains are optokinetically blind, i.e. they do not react to optokinetic stimulation at all (Lannou et al. 1982; Collewijn et al. 1985; Mangini et al. 1985; Garipis and Hoffmann 1999). Electrophysiologically, these defects are reflected by the lack of direction selectivity of neurons in the NOT-DTN (Lannou et al. 1982) or by reversed direction selectivity in these neurons (Winterson and Collewijn 1981). Anatomically, the most prominent characteristic is the severe reduction of the ipsilateral retinofugal projections (rat: Lund 1965; Aarnoutse et al. 1995; ferret: Cucchiaro and Guillery 1984; Morgan and Thompson 1985; Morgan et al. 1987; cat: Guillery and Kaas 1971, 1973; Hubel and Wiesel 1971). Anatomical tract tracing experiments have shown that the ipsilateral retinal projections to the NOT-DTN and the accessory optic system are largely lost in the albino ferret (Zhang and Hoffmann 1993). In the NOT-DTN of albino ferrets, retinal slip neurons can be identified through

their projection to the IO. However, these cells have lost their characteristic preference for ipsiversive stimulus movement. This physiological abnormality results in the more or less complete loss of optokinetic eye movements in albino ferrets (Garipis and Hoffmann 1999).

How can we relate these findings to our present anatomical results? There was no significant difference in the total number of NOT-DTN to IO projecting cells in normal and albino ferrets. This reflects the fact that in electrophysiological experiments retinal slip neurons could be identified by antidromic stimulation in the IO (Garipis and Hoffmann 1999).

Can we explain the loss of direction selectivity? As has been argued for the rabbit and shown in the cat, direction selective ganglion cells provide the retinal input to the NOT-DTN (Oyster et al. 1972; Hoffmann and Stone 1985). Rotation of the eye around the torsional axis in wallabies suggests that retinal coordinates (and retinal direction selectivity) determine the direction selectivity in the NOT-DTN (Hoffmann et al. 1995). Extrapolating these findings to the ferret, one has to assume that a putative reduction of retinal direction selectivity could cause the reduction of direction selective responses in the albino NOT-DTN. To test this hypothesis, one will have to compare the incidence of direction selective neurons in the retina of pigmented and albino ferrets. In addition, the abnormally crossing ganglion cell axons from the temporal retina can produce non-congruent visual field maps in visual centres, thus causing non-matching retinal inputs to the target cells (Guillery 1990).

Our results show that the retinal slip cells of albino animals have fewer stem dendrites and a drastically reduced cumulative dendritic length. In addition, the conspicuous dendritic network in the NOT-DTN of pigmented ferrets is largely lost in the albino. It is well known that the dendritic growth is remarkably dynamic and responsive to environmental signals including guidance molecules and levels and patterns of activity (for review see McAllister 2000). There is compelling evidence that dendritic branches are stabilized and stimulated to grow by synaptic contacts during normal development (Vaughn 1989), determining their size and complexity (Purves and Hume 1981; Purves and Lichtman 1985). On the other hand, decreasing or blocking afferent activity often results in stunted neuronal development and dendritic retraction (Wiesel and Hubel 1963; Guillery 1973; Deitch and Rubel 1984). Both the genetically determined and activity-dependent formation of dendrites are mediated by a number of substrate-bound or soluble factors including neurotransmitters, neurotrophins, etc., that act to enhance or inhibit their growth (Snider 1988; McAllister et al. 1996; Lom and Cohen-Cory 1999). The expression of these factors is specific to their tissue of origin, physiological state and age (McAllister et al. 1999; for review see Keith and Wilson 2001). Many of the molecular signals that influence dendritic growth also regulate axon guidance and synapse formation and their expression levels are modulated by synaptic activity (McAllister 2000). Thus, we can hypothesize that possibly a decreased or unstructured input in a critical phase during development could cause the reduction in stem dendrite growth and neuropil in the albino NOT-DTN. In addition, the occurrence of factors which are important regulators of dendritic development could be different in the brains of normally pigmented and albino animals. All these hypotheses await further investigation.

Interestingly, morphological studies in the auditory brainstem, especially in the medial superior olivary nucleus of albino rabbits, cats, and ferrets, have also revealed reduced soma sizes and reduced overall dendritic length in albino versus pigmented animals (Conlee et al. 1984, 1987; Baker and Guillery 1989). A developmental study further showed that these morphological differences only developed in ferrets older than 6 months of age (Baker and Guillery 1989). Because all our animals were older than 6 months and the two groups were age matched, this developmental course should not influence our data. The morphological changes in the superior olive and the NOT-DTN have clear functional correlates: obliteration of the auditory brainstem response in the auditory system and optokinetic blindness in the visual system (Creel et al. 1983; Garipis and Hoffmann 1999). Electrophysiological data on the primary somatosensory cortex of albino cats did not reveal any obvious abnormalities in somatotopy (Garraghty et al. 1990). Thus, the effects of albinism seem to be especially disastrous on the subcortical level. Whether the somatosensory system is also affected on this level remains to be investigated.

Furthermore, at least in the pigmented ferret, a cortical input to the NOT-DTN has been demonstrated (Klauer et al. 1990; Zhang 1991). The IO-projecting NOT-DTN neurons lie in the terminal fields of cortical afferents (Zhang 1991). Assuming that in the ferret as in the monkey (Hoffmann et al. 1991) cortical projection neurons to the NOT-DTN, as a population, match the directional preference of their target cells, we could expect from a loss of direction selectivity in the NOT-DTN a loss in specificity or a reduction in the cortical projection to the NOT-DTN. Preliminary data from our laboratory show that neurons in the visual cortex of albino ferrets have normal direction selectivity (Garipis and Hoffmann, unpublished). This would imply that direction selectivity of the cortical projection to the NOT-DTN alone is not sufficient to establish the appropriate selectivity for ipsiversive movement in the NOT-DTN. Based on the Hebbian rule, one can speculate that only synapses of cortical axons with similar directional preferences as the NOT-DTN cells will be consolidated during development. If the postsynaptic target neurons are not direction selective, the specificity of coinciding activity is reduced, and cortical synapses may not be consolidated. This, in turn, could then accentuate the loss of inputs to the NOT-DTN. This hypothesis would have to be tested using electron microscopy to compare the incidence of synapses on IO-projecting neurons in normal and albino ferrets.

In conclusion, our data indicate that a clear defect in the optokinetic system of albino ferrets is located in the first retinofugal relay station in the subcortical pathway under-

lying the optokinetic reflex, namely the NOT-DTN. Further experiments will have to discern whether this defect is caused by retinal mechanisms, i.e. decreased ganglion cell density, loss of direction selectivity in retinal ganglion cells, or axonal misrouting in the optic chiasm, or whether a loss of cortical or intrinsic inputs plays the crucial role.

Acknowledgements We thank E. Brockmann for expert technical assistance, I. Paas and S. Krämer for the photography, and Dr. C. Distler for her helpful input to this paper. This study was supported by the Deutsche Forschungsgemeinschaft through a scholarship of the Graduate Program KOGNET to I.T.

References

Aarnoutse EJ, van der Want JJL, Vrensen GFJM (1995) Retrograde fluorescent microsphere tracing of retinal and central afferents to the nucleus of the optic tract in pigmented and albino rats. Neurosci Lett 201:143–146

Baker GE, Guillery RW (1989) Evidence for the delayed expression of a brainstem abnormality in albino ferrets. Exp Brain Res 74:658–662

Ballas I, Hoffmann K-P (1985) A correlation between receptive field properties and morphological structures in the pretectum of the cat. J Comp Neurol 238:417–428

Ballas I, Hoffmann K-P, Wagner HJ (1981) Retinal projection to the nucleus of the optic tract in the cat as revealed by retrograde transport of horseradish peroxidase. Neurosci Lett 26:197–202

Bandtlow CE, Zimmermann DR (2000) Proteoglycans in the developing brain: new conceptual insights for old proteins. Physiol Rev 80:1267–1290

Büttner-Ennever JA, Cohen B, Horn AKH, Reisine H (1996a) Pretectal projections to the oculomotor complex of the monkey and their role in eye movements. J Comp Neurol 366:348–359

Büttner-Ennever JA, Cohen B, Horn AKH, Reisine H (1996b) Efferent pathways of the nucleus of the optic tract in monkey and their role in eye movements. J Comp Neurol 373:90–107

Cazin L, Precht W, Lannou J (1980) Pathways mediating optokinetic responses of vestibular nucleus neurons in the rat. Pflugers Arch 384:19–29

Collewijn H (1975a) Oculomotor areas in the rabbit's midbrain and pretectum. J Neurobiol 6:3–22

Collewijn H (1975b) Direction-selective units in the rabbit's nucleus of the optic tract. Brain Res 100:489–508

Collewijn H, Winterson BJ, Dubois MFW (1978) Optokinetic eye movements in albino rabbits: inversion in anterior visual field. Science 199:1351–1353

Collewijn H, Apkarian P, Spekreijse H (1985) The oculomotor behaviour of human albinos. Brain 108:1–28

Conlee JW, Parks TN, Romero C, Creel DJ (1984) Auditory brainstem anomalies in albino cats. II. Neuronal atrophy in the superior olive. J Comp Neurol 225:141–148

Conlee JW, Parks TN, Creel DJ (1987) Reduced neuronal size and dendritic length in the medial superior olivary nucleus of albino rabbits. Brain Res 363:28–37

Creel D, Conlee JW, Parks TN (1983) Auditory brainstem anomalies in albino cats. I. Evoked potential studies. Brain Res 260:1–9

Cucchiaro J, Guillery RW (1984) The development of retinogeniculate pathways in normal and albino ferrets. Proc R Soc Lond B 223:141–164

Deitch JS, Rubel EW (1984) Afferent influences on brain stem auditory nuclei of the chicken: the time course and specificity of dendritic atrophy following deafferentation. J Comp Neurol 229:66–79

Gallyas F, Merchenthaler I, Liposits Z (1993) Silver-gold intensification of diaminobenzidine immunoreaction product for light and electron microscopy. Neurosci Protocols 50:1–11

Garipis N, Hoffmann K-P (1999) Changes in the neuronal circuit of the horizontal optokinetic reflex in albino ferrets. In: Elsner N, Eysel U (eds) From molecular neurobiology to clinical neuroscience. Proc 11th Göttingen conference of German Neuroscience Soc, vol 1, Thieme, Stuttgart, p 475

Garraghty PE, Schall JD, Kaas JH (1990) Normal somatotopy in SI of a tyrosinase-negative albino cat. Brain Res 536:315–317

Giolli RA, Blanks RHI, Torigoe Y (1984) Pretectal and brainstem projections of the medial terminal nucleus of the accessory optic system of the rabbit and the rat as studied by anterograde and retrograde neuronal tracing methods. J Comp Neurol 227:228–251

Grasse KL, Cynader MS (1990) The accessory optic system of frontal-eyed animals. In: Leventhal A (ed) Vision and visual dysfunction, vol IV. The neuronal basis of visual function. Macmillan, Basingstoke, pp 111–137

Graybiel AM, Berson DM (1980) Autoradiographic evidence for a projection from the pretectal nucleus of the optic tract to the dorsal lateral geniculate complex in the cat. Brain Res 195:1–12

Gregory KM (1985) The dendritic architecture of the visual pretectal nuclei of the rat: a study with the Golgi-Cox method. J Comp Neurol 234:122–135

Greiner JV, Weidman TA (1981) Histogenesis of the ferret retina. Exp Eye Res 33:315–332

Guillery RW (1971) An abnormal retinogeniculate projection in the albino ferret (*Mustela furo*). Brain Res 33:482–485

Guillery RW (1973) Quantitative studies of transneuronal atrophy in the dorsal lateral geniculate nucleus of cats and kittens. J Comp Neurol 148:423–438

Guillery RW (1990) Normal and abnormal visual field maps in albinos. Central effects of non-matching maps. Ophthal Paed Genet 11:177–183

Guillery RW, Kaas JH (1971) A study of normal and congenitally abnormal retinogeniculate projections in cats. J Comp Neurol 143:73–100

Guillery RW, Kaas JH (1973) Genetic abnormality of the visual pathways in a "white" tiger. Science 180:1287–1289

Hein A, Courjon JH, Flandrin JM, Arzi M (1990) Optokinetic nystagmus in the ferret: including selected comparisons with the cat. Exp Brain Res 79:623–632

Hoffmann K-P (1982) Cortical versus subcortical contributions to the optokinetic reflex in the cat. In: Lennerstand G, Zee S, Keller EL (eds) Functional basis of ocular motility disorders. Pergamon, New York, pp 303–310

Hoffmann K-P, Fischer WH (2001) Directional effect of inactivation of the nucleus of the optic tract on optokinetic nystagmus in the cat. Vision Res (in press)

Hoffmann K-P, Stone J (1985) Retinal input to the nucleus of the optic tract of the cat assessed by antidromic activation of ganglion cells. Exp Brain Res 59:395–403

Hoffmann K-P, Behrend K, Schoppmann A (1976) A direct efferent visual pathway from the nucleus of the optic tract to the inferior olive in the cat. Brain Res 115:150–153

Hoffmann K-P, Distler C, Erickson RG, Mader W (1988) Physiological and anatomical identification of the nucleus of the optic tract and dorsal terminal nucleus of the accessory optic system in monkeys. Exp Brain Res 69:635–644

Hoffmann K-P, Distler C, Erickson R (1991) Functional projections from striate cortex and superior temporal sulcus to the nucleus of the optic tract (NOT) and dorsal terminal nucleus of the accessory optic tract (DTN) of macaque monkeys. J Comp Neurol 313:707–724

Hoffmann K-P, Distler C, Mark R, Marotte LR, Henry GH, Ibbotson MR (1995) Neural and behavioral effects of early eye rotation on the optokinetic system in the wallaby, *Macropus eugenii*. J Neurophysiol 73:727–735

Holstege G, Collewijn H (1982) The efferent connections of the nucleus of the optic tract and the superior colliculus in the rabbit. J Comp Neurol 209:139–175

Horn AKE, Hoffmann K-P (1987) Combined GABA-immunocytochemistry and TMB-HRP histochemistry of pretectal nuclei projecting to the inferior olive in rats, cats and monkeys. Brain Res 409:133–138

Huang K, Guillery RW (1985) A demonstration of two distinct geniculocortical projection patterns in albino ferrets. Dev Brain Res 20:213–220
Hubel DH, Wiesel TN (1971) Aberrant visual projections in the Siamese cat. J Physiol 218:33–62
Ibbotson MR, Mark RF, Maddess TL (1994) Spatiotemporal response properties of direction-selective neurons in the nucleus of the optic tract and dorsal terminal nucleus of the wallaby, *Macropus eugenii*. J Neurophysiol 72:2927–2943
Ilg UJ, Bremmer F, Hoffmann K-P (1993) Optokinetic and pursuit system: a case report. Behav Brain Res 57:21–29
Itoh K (1977) Efferent projections of the pretectum in the cat. Exp Brain Res 50:89–105
Jeffery G (1997) The albino retina: an abnormality that provides insight into normal retinal development. Trends Neurosci 20:165–169
Kato I, Harada K, Hasegawa T, Ikarashi T (1986) Role of the nucleus of the optic tract in monkey in relation to optokinetic nystagmus. Brain Res 364:12–22
Keith CH, Wilson MT (2001) Factors controlling axonal and dendritic arbors. Int Rev Cytol 205:77–147
Klauer S, Sengpiel F, Hoffmann K-P (1990) Visual response properties and afferents of the nucleus of the optic tract in the ferret. Exp Brain Res 83:178–189
Lannou J, Cazin L, Precht W, Toupet M (1982) Optokinetic, vestibular, and optokinetic-vestibular responses in albino and pigmented rats. Pflugers Arch 393:42–44
Law MI, Zahs KR, Stryker MP (1988) Organization of primary visual cortex (area 17) in the ferret. J Comp Neurol 278:157–180
Lom B, Cohen-Cory S (1999) Brain-derived neurotrophic factor differentially regulates retinal ganglion cell dendritic and axonal arborization *in vivo*. J Neurosci 19:9928–9938
Lund RD (1965) Uncrossed visual pathways of hooded and albino rats. Science 149:1506–1507
Magnin M, Kennedy H, Hoffmann K-P (1989) A double-labeling investigation of the pretectal visuo-vestibular pathways. Visual Neurosci 3:53–58
Mangini NJ, Vanable JW, Williams MA, Pinto LH (1985) The optokinetic nystagmus and ocular pigmentation of hypopigmented mouse mutants. J Comp Neurol 241:191–209
McAllister AK (2000) Cellular and molecular mechanisms of dendrite growth. Cereb Cortex 10:963–973
McAllister AK, Lo DC, Katz LC (1996) Neurotrophins regulate dendritic growth in developing visual cortex. Neuron 15:791–803
McAllister AK, Katz LC, Lo DC (1999) Neurotrophins and synaptic plasticity. Ann Rev Neurosci 22:295–318
Mesulam MM (1978) Tetramethylbenzidine for horseradish peroxidase neurohistochemistry: a non-carcinogenic blue reaction product with superior sensitivity for visualisation of neuron afferents and efferents. J Histochem Cytochem 26:123–131
Montero VM, Guillery RM (1978) Abnormalities of the corticogeniculate pathway in Siamese cats. J Comp Neurol 179:1–12
Morgan JE, Thompson ID (1985) The distribution of ipsilaterally projecting ganglion cells in neonatal pigmented and albino ferrets. J Physiol (Lond) 369:35
Morgan JE, Henderson Z, Thompson ID (1987) Retinal decussation patterns in pigmented and albino ferrets. Neuroscience 2:519–535
Mustari MJ, Fuchs AF, Kaneko CRS, Robinson FR (1994) Anatomical connections of the primate nucleus of the optic tract. J Comp Neurol 349:111–128
Neuhauss SC, Biehlmaier O, Seeliger MW, Das T, Kohler K, Harris WA, Baier H (1999) Genetic disorders of vision revealed by a behavioral screen of 400 essential loci in zebrafish. J Neurosci 19:8603–8615
Oyster CW, Takahashi E, Collewijn H (1972) Direction-selective retinal ganglion cells and control of optokinetic nystagmus in the rabbit. Vision Res 12:183–193
Precht W, Cazin L (1979) Functional deficits in the optokinetic system of albino rats. Exp Brain Res 37:183–186
Precht W, Strata P (1980) On the pathway mediating optokinetic responses in vestibular nuclear neurons. Neuroscience 5:777–787
Purves D, Hume RI (1981) The relation of postsynaptic geometry to the number of presynaptic neurons that innervate autonomic ganglion cells. J Neurosci 1:441–452
Purves D, Lichtman JW (1985) Geometrical differences among homologous neurons in mammals. Science 228:298–302
Schiff D, Cohen B, Raphan T (1988) Nystagmus induced by stimulation of the nucleus of the optic tract in the monkey. Exp Brain Res 79:1–14
Schiff D, Cohen B, Büttner-Ennever J, Matsuo V (1990) Effects of lesions of the nucleus of the optic tract on optokinetic nystagmus and afternystagmus in the monkey. Exp Brain Res 79:225–239
Schmidt M, Schiff D, Bentivoglio M (1995) Independent efferent populations in the nucleus of the optic tract: an anatomical and physiological study in rat and cat. J Comp Neurol 360:271–285
Simpson JI (1984) The accessory optic system. Ann Rev Neurosci 7:13–41
Sirkin DW, Hess BJM, Precht W (1985) Optokinetic nystagmus in albino rats depends on stimulus pattern. Exp Brain Res 61:218–221
Snider WD (1988) Nerve growth factor enhances dendritic arborization of sympathetic ganglion cells in developing mammals. J Neurosci 8:2628–2634
Takeda T, Maekawa K (1976) The origin of the pretecto-olivary tract. A study using the horseradish peroxidase method. Brain Res 117:319–325
Terasawa K, Otani K, Yamada J (1979) Descending pathways of the nucleus of the optic tract in the rat. Brain Res 173:405–417
Thompson ID (1990) Retinal pathways and the developmental basis of binocular vision. In: Blakemore C (ed) Vision: coding and efficiency. Cambridge University Press, Cambridge, pp 209–223
van der Togt C, van der Want J (1992) Variation in form and axonal termination in the nucleus of the optic tract of the rat: the medial terminal nucleus input on neurons projecting to the inferior olive. J Comp Neurol 325:446–461
van der Want JJL, Klooster J, Nunes Cardozo B, de Weerd H, Liem RSB (1997) Tract-tracing in the nervous system of vertebrates using horseradish peroxidase and its conjugates: tracers, chromogens, and stabilization for light and electron microscopy. Brain Res Protocols 1:269–279
Vargas CD, Volchan E, Nasi JP, Bernardes RF, Rocha-Miranda CE (1996) The nucleus of the optic tract (NOT) and the dorsal terminal nucleus (DTN) of opossums (*Didelphis marsupialis aurita*). Brain Behav Evol 48:1–15
Vaughn JE (1989) Fine structure of synaptogenesis in the vertebrate central nervous system. Synapse 3:255–285
Walberg F, Nordby T, Hoffmann K-P, Hollaender H (1981) Olivary afferents from the pretectal nuclei in the cat. Anat Embryol 161:291–304
Wallman J (1993) Subcortical optokinetic mechanisms. In: Miles FA, Wallman J (eds) Visual motion and its role in the stabilization of gaze. Elsevier, Amsterdam, pp 321–342
Wiesel TN, Hubel DH (1963) Effects of visual deprivation on morphology and physiology of cells in the cat's lateral geniculate body. J Neurophysiol 26:978–993
Winterson BJ, Collewijn H (1981) Inversion of direction-selectivity to anterior fields in neurons of nucleus of the optic tract in rabbits with ocular albinism. Brain Res 220:31–49
Wood CC, Spear PD, Braun JJ (1973) Direction-specific deficits in horizontal optokinetic nystagmus following removal of visual cortex in the cat. Brain Res 60:231–237
Zee DS, Tusa RJ, Herdman SJ, Butler PH, Gücer G (1987) Effects of occipital lobectomy upon eye movement in primate. J Neurophysiol 58:883–907
Zhang HY (1991) Neuroanatomische Grundlagen des optokinetischen Nystagmus bei Säugetieren. PhD thesis, Ruhr University, Bochum
Zhang HY, Hoffmann K-P (1993) Retinal projections to the pretectum, accessory optic system and superior colliculus in pigmented and albino ferrets. Eur J Neurosci 5:486–500